



# Investigating and controlling the quantum resources of bipartite-qubit detectors of scalar fields in the process of spacetime expansion

Huan Yang<sup>1,a</sup>, Ling-Ling Xing<sup>1</sup>, Min Kong<sup>1</sup>, Gang Zhang<sup>1,b</sup>, Liu Ye<sup>2</sup>

<sup>1</sup> School of Electrical and Photoelectronic Engineering, West Anhui University, Lu'an 237012, China

<sup>2</sup> School of Physics and Optoelectronic Engineering, Anhui University, Hefei 230601, China

Received: 21 March 2023 / Accepted: 15 October 2023 / Published online: 26 October 2023  
© The Author(s) 2023

**Abstract** Quantum resources construct new avenues to explore the cosmos. Considering bipartite-qubit detectors subjected to scalar fields in an expanding spacetime, quantum resources (including quantum coherence, quantum discord, Bell-nonlocality, and nonlocal advantage of quantum coherence) of the system are characterized. The influences of various cosmic parameters on these quantum resources are investigated. Besides, we use the filtering operation to propose a strategy that can be used to control these quantum resources. The results reveal that quantum coherence and quantum discord can not disappear at different expansion rapidity, expansion volumes, and particle masses of scalar field. Conversely, one can not capture Bell-nonlocality and nonlocal advantage of quantum coherence at higher expansion rapidity, larger expansion volume, and smaller particle mass. The dissipation of quantum resources can be resisted via the filtering operation. One can use the filtering operation to remarkably strengthen these quantum resources of the system.

## 1 Introduction

Quantum resources are the significant traits of quantum field, and they embody differently crucial application values in quantum information science [1]. Quantum coherence (QC) is a fundamental quantum resource, and it stems from the fluctuation of microscopic particles. QC investigation can be traced backed to its quantification framework [2]. Based on a fixed reference basis, a series of QC measurements were proposed, including the relative entropy of coherence [2], the

$l_1$  norm of coherence [2], the skew information of coherence [3–5], and the robustness of coherence [6, 7]. QC becomes a promising topic in quantum channel discrimination, quantum thermodynamics, quantum metrology, and quantum algorithms [8, 9]. There have been valuable efforts to improve QC [10–15].

Quantum properties of nonclassical correlations of two-qubit systems can be quantified through the quantum discord (QD) [16, 17]. It is deemed as the difference between total correlation and classical correlation [16, 17]. The previous results indicated that some separable states with QD can be used to realize quantum information tasks. Examples include state discrimination [18, 19], quantum computation [20], Grover search [21], and quantum phase transitions [22, 23]. Bell-nonlocality (BN) is found to be a stricter criterion for predicting quantum correlation when compared to both QC and QD. For a bipartite state, BN describes the nonlocality that the joint probability distributions of arbitrary measurement outcomes can not be represented by local hidden variable-local hidden variable model [24, 25]. The violation of the Bell inequality (for example Clauser–Horne–Shimony–Holt (CHSH) inequality [26]) manifests that the bipartite state possesses BN. BN plays a nontrivial role in the field of quantum information [27–29].

In particular, the nonlocal advantage of quantum coherence (NAQC) was proposed by Mondal et al. as a new quantum resource [30]. NAQC reveals the nonclassical phenomenon that the upper bound of QC quantified under a set of mutually unbiased bases for a single-qubit state can be punctured by performing a local measurement on a bipartite system [30]. One can achieve NAQC by employing different criteria, which relies on the measure of QC. A variety of valuable achievements have been obtained in the related efforts [31–34]. Also, Ding et al. verified NAQC of two-qubit states

<sup>a</sup> e-mail: [hyang80@163.com](mailto:hyang80@163.com) (corresponding author)

<sup>b</sup> e-mail: [zhanggang@wxc.edu.cn](mailto:zhanggang@wxc.edu.cn)

in experiment [35], and this work establishes a base for the practical application of NAQC.

Due to the ubiquitous and remarkable applications of these quantum resources in the field of quantum information area, the explorations regarding QC, QD, BN, and NAQC in different models are always hot topics. Recently, the quantum resources have been used to cognize the nonclassical traits of various systems. Involving two-level molecular systems [36], quantum batteries [37, 38], dilaton spacetime [39], neutrino oscillations [40–43], curved space-time [44], fermion systems [45], noninertial frame [46], and black holes [47].

Significantly for what follows, the expanding spacetime is an essential model that can be used to explore the cosmos. Some concepts of quantum information have been used to investigate expanding spacetime [48–57], and the quantum resources reveal a new avenue to cognize the cosmos. To be clearer, relevant efforts can help us predicting the particle creation in an expanding spacetime [49], capture spacetime curvature [51], and demonstrate the influences of cosmic parameters on the quantum entanglement of the system [55]. However, explorations regarding QC, QD, BN, and NAQC of two-qubit detector subjected to scalar fields in an expanding spacetime are still lacking. Meanwhile, the controls and enhancements of these quantum resources of two-qubit detectors subjected to scalar fields in an expanding spacetime have not been achieved till now. These explorations can shed new light on the cosmos from the perspective of quantum information, and provide a vital technique to steer the quantum resources of bipartite-qubit detectors subjected to scalar fields in an expanding spacetime.

Enlightened by this, our attention is directed to characterize QC, QD, BN, and NAQC of two-qubit detectors subjected to scalar fields in an expanding spacetime, and explore the effects of different cosmic parameters on QC, QD, BN, and NAQC. Moreover, we design a scheme that can be used to control the quantum resources of two-qubit detectors subjected to scalar fields in an expanding spacetime. It is revealed that an increase in the expansion rapidity gives rise to the decreases in QC, QD, BN, and NAQC. High expansion rapidity is responsible for the invariant traits of QC and QD. NAQC and BN can not be detected when the volume expansion approaches the maximum or the particle mass of the scalar field is small. An increase in the mass of the scalar field particle results in invariance of QC, QD, BN, and NAQC. The influences of different cosmic parameters on quantum resources can be controlled through the filtering operation. One can use the operation to battle against the declines of quantum resources of two-qubit detectors subjected to scalar fields in an expanding spacetime. The quantum resources can be achieved with the help of the filtering operation in the cases of higher expansion rapidity, stronger volume expansion, and smaller particle mass.

In Sect. 2, the model of two-qubit detectors coupled to scalar fields is provided. QC, QD, BN, and NAQC of the system are characterized in Sect. 3. Also, the effects of different cosmic parameters on QC, QD, BN, and NAQC are investigated in this section. Section 4 reveals the avenue that can be used to control the quantum resources of two-qubit detectors subjected to scalar fields in an expanding spacetime. Finally, conclusions are drawn.

## 2 Bipartite-qubit detectors subjected to scalar fields in an expanding spacetime

We consider a Robertson–Walker metric,  $ds^2 = R(\eta)^2(d\eta^2 - dx^2)$ , where  $\eta$  ( $-\infty < \eta < +\infty$ ) is the conformal time and  $R(\eta)^2$  ( $R(\eta) = \sqrt{1 + \varepsilon[1 + \tanh(\sigma\eta)]}$ ) is the conformal scale factor [48, 58]. The volume expansion and expansion rapidity of spacetime are  $\varepsilon$  and  $\sigma$ , respectively.  $\eta \rightarrow -\infty$  and  $R(\eta)^2 = 1$  ( $\eta \rightarrow +\infty$  and  $R(\eta)^2 = 1 + 2\varepsilon$ ) indicate the distant past (the far future) for the flat space-time.

A real scalar field  $\Phi(x, \eta)$  satisfies Klein–Gordon equation, i.e.,  $(\square + m^2)\Phi = 0$  ( $\square\Phi = \partial_\mu(\sqrt{-g}g^{\mu\nu}\partial_\nu\Phi)/\sqrt{-g}$ ), where  $\Phi(x, \eta) = (2\pi\omega_k)^{-1/2}e^{ikx}\xi_k(\eta)$  [58, 59] with equation  $\partial_\eta^2\xi_k(\eta) + [k^2 + R^2(\eta)m^2]\xi_k(\eta) = 0$ . When  $\eta \rightarrow -\infty$  and  $\eta \rightarrow +\infty$ , we respectively label two solutions of the equation as  $\mu_k^{in}$  and  $\mu_k^{out}$ . The relation between  $\mu_k^{in}$  and  $\mu_k^{out}$  is [58, 59]

$$\mu_k^{in}(x, \eta) = \alpha_k\mu_k^{out}(x, \eta) + \beta_k\mu_{-k}^{out*}(x, \eta), \tag{1}$$

where  $\alpha_k$  and  $\beta_k$  ( $|\alpha_k|^2 - |\beta_k|^2 = 1$ ) are the Bogoliubov coefficients, given by

$$\alpha_k = \left(\frac{\omega_{out}}{\omega_{in}}\right)^{\frac{1}{2}} \frac{\Gamma\left(1 - \frac{i\omega_{in}}{\sigma}\right)\Gamma\left(-\frac{i\omega_{out}}{\sigma}\right)}{\Gamma\left(-\frac{i\omega_{+}}{\sigma}\right)\Gamma\left(1 - \frac{i\omega_{+}}{\sigma}\right)}, \tag{2}$$

$$\beta_k = \left(\frac{\omega_{out}}{\omega_{in}}\right)^{\frac{1}{2}} \frac{\Gamma\left(1 - \frac{i\omega_{in}}{\sigma}\right)\Gamma\left(\frac{i\omega_{out}}{\sigma}\right)}{\Gamma\left(\frac{i\omega_{-}}{\sigma}\right)\Gamma\left(1 + \frac{i\omega_{-}}{\sigma}\right)}. \tag{3}$$

$\omega_{out} = [k^2 + m^2(1 + 2\varepsilon)]^{1/2}$ ,  $\omega_{in} = (k^2 + m^2)^{1/2}$ , and  $\omega_{\pm} = (\omega_{out} \pm \omega_{in})/2$ . In the following sections, we have taken all parameters (including expansion rapidity  $\sigma$  and energy level  $\Omega$ ) in units of the momentum  $k$ , and  $k = 1$  is assumed for simplicity. One can use

$$\aleph_k = \left|\frac{\beta_k}{\alpha_k}\right|^2 = \frac{\sinh^2(\pi\omega_{-}/\sigma)}{\sinh^2(\pi\omega_{+}/\sigma)} \tag{4}$$

to indicate the mixed degree between  $\mathbf{k}$  and  $-\mathbf{k}$  (the “in” modes). Besides,  $|\beta_k|^2 = 1/(\aleph_k^{-1} - 1)$  [49] represents the average particle number of “out” modes [49].  $\aleph_k \rightarrow 0$  ( $\aleph_k \rightarrow 1$ ) induces  $|\beta_k|^2 \rightarrow 0$  ( $|\beta_k|^2 \rightarrow \infty$ ). The creation and annihilation operators are [60]

$$\hat{a}_k^{in} = \alpha_k^* \hat{a}_k^{out} - \beta_k^* \hat{a}_{-k}^{out\dagger}, \tag{5}$$

$$\hat{a}_k^{in\dagger} = \alpha_k \hat{a}_k^{out\dagger} - \beta_k \hat{a}_{-k}^{out}. \tag{6}$$

The “in” vacuum in the sectors of the (unordered) pair  $\mathbf{k}$  and  $-\mathbf{k}$  is [55]

$$|0\rangle_k^{in} |0\rangle_{-k}^{in} = \sum_n A_{n,k} |0\rangle_k^{out} |0\rangle_{-k}^{out} \tag{7}$$

with

$$A_{n,k} = \left(\frac{\beta_k^*}{\alpha_k^*}\right)^n \sqrt{1 - \varkappa_k}, \tag{8}$$

where  $n$  is the particle content. In opposite directions, each pair of modes keeps away from the other [49]. The state of mode  $\mathbf{k}$  is [55]

$$\begin{aligned} \rho_k^{out} &= Tr_{-k} [|0\rangle_k^{in} |0\rangle_{-k}^{in} \langle 0|_k^{in} \langle 0|] \\ &= (1 - \varkappa_k) \sum_n \varkappa_k^n |n\rangle_k \langle n|, \end{aligned} \tag{9}$$

where  $|n\rangle_k \langle n|$  is a stenography for  $|n\rangle_k^{out} \langle n|_k^{out}$ .

In the far future of the expanding spacetime (described by Eq. (2)), considering the Unruh–DeWitt (UDW) detector model [61] in which the detector locally subjected to scalar fields. The UDW detectors can be modelled by nonlinear optics system [62], electro-optic sampling of the electromagnetic vacuum [63], coupled laser field [64], and two-level atomic or artificial-atom systems [65]. The Hamiltonian is [55]

$$\hat{H} = \hat{H}_q + \hat{H}_\Phi + \hat{H}_I. \tag{10}$$

$\hat{H}_q = \Omega \hat{\Upsilon}^\dagger \hat{\Upsilon}$  ( $\Omega$  is the energy level difference between  $|0\rangle$  and  $|1\rangle$ .  $\hat{\Upsilon}^\dagger$  and  $\hat{\Upsilon}$  are the rising and lowering operators, respectively.) is the Hamiltonian for the qubit detector.  $\hat{H}_\Phi$  is the Klein–Gordon Hamiltonian of the scalar field.  $\hat{H}_I(t) = \zeta(t) \int_\Sigma \Phi(x, t) [\psi(x) \hat{\Upsilon} + \psi^*(x) \hat{\Upsilon}^\dagger] \sqrt{-g} dx$  is the interaction.  $\psi(x)$  ( $\zeta(t)$ ) is a smooth function (the coupling constant with a finite duration of qubit-field interaction).  $\Sigma$  is the spacelike Cauchy surface.

$$U \approx 1 + i \hat{\Upsilon} \hat{a}^\dagger(\Gamma^*) - i \hat{\Upsilon}^\dagger \hat{a}(\Gamma^*) \tag{11}$$

is the unitary transformation induced by the Hamiltonian [61]. Here,  $\Gamma(x) = -2i \int \vartheta \psi^*(x') \sqrt{-g'} d^2x'$ ,  $\vartheta = [G_R(x; x') - G_A(x; x')] \times \zeta(t') e^{i\Omega t'}$ .  $\hat{a}(\Gamma^*) |n\rangle_k = \sqrt{n} \mu_k |n-1\rangle_k$ ,  $\hat{a}^\dagger(\Gamma^*) |n\rangle_k = \sqrt{n+1} \mu_k^* |n+1\rangle_k$ , and  $\mu_k = \langle \Gamma_q^*, \chi_k \rangle$  [61].

The single mode approximation is taken, which is valid only in a certain regime. That is, the coupling between the detector qubit and the mode  $\mathbf{k}_0$  is dominant, however, the coupling between the detector qubit and other field modes are weak ( $-\mathbf{k}_0$  is out of access because of the separation on a cosmological scale) [55]. In this regime, the coupling between the detector qubit and all the field modes can be

ignored, and only the interaction between the detector qubit and the field mode  $\mathbf{k}_0$  (the energy is  $\Omega$ ) can be considered [55]. The purpose of using the single mode approximation is to obtain the influence between the mode  $\mathbf{k}_0$  and the detector qubit, namely [55],

$$\begin{aligned} |n\rangle \otimes |0\rangle &\rightarrow |n\rangle \otimes |0\rangle - i \sqrt{n} \mu |n-1\rangle \otimes |1\rangle, \\ |n\rangle \otimes |1\rangle &\rightarrow |n\rangle \otimes |1\rangle + i \sqrt{n+1} \mu^* |n+1\rangle \otimes |0\rangle, \end{aligned} \tag{12}$$

where we omit the mode index  $\mathbf{k}_0$  of the Fock state  $|n\rangle$  and the inner product of the mode functions  $\mu = \langle \Gamma_q^*, \chi_{k0} \rangle$  [55].  $m\sqrt{1+2\varepsilon}$  is the minimum energy of a particle generated in expansion spacetime.  $\omega_{out} = \sqrt{k^2 + m^2(1+2\varepsilon)} \geq m\sqrt{1+2\varepsilon}$ .  $\Omega \geq m\sqrt{1+2\varepsilon}$  must be satisfied due to the fact that the field modes can influence the qubit. Therefore,  $\varepsilon \leq \varepsilon_{max} = (\Omega^2/m^2 - 1)/2$  [55]. Of particular note is that  $\varepsilon_{max}$  is the maximum volume such that our approximation can give any meaningful results, with results only being trustworthy for  $\varepsilon \ll \varepsilon_{max}$ . The  $\varepsilon_{max}$  is a detector dependent quantity, and not a fundamental property of spacetime.

Here, we consider the model in which the created particles in the expansion spacetime constitute the surrounding environment of a two-entangled-qubit detector [55]. The entangled-qubit can be realized by different physical systems, including quantum dot system [66–68], Heisenberg spin chains system [69–72], superconducting system [73–75], cavity QED system [76–78], and Rydberg atom system [79–81]. The initial state of a two-entangled-qubit detector is  $|\psi\rangle = \cos \theta |01\rangle + \sin \theta |10\rangle$ . When one of the qubits is coupled to a scalar field, the other one is decoupled [55]. Under the basis of  $\{|00\rangle, |01\rangle, |10\rangle, |11\rangle\}$  (namely, under the  $\sigma_z$ -representation), the final state of the two-qubit detector is [55]

$$\rho_{AB} = \begin{pmatrix} \rho_{11} & 0 & 0 & 0 \\ 0 & \rho_{22} & \rho_{23} & 0 \\ 0 & \rho_{32} & \rho_{33} & 0 \\ 0 & 0 & 0 & \rho_{44} \end{pmatrix}, \tag{13}$$

with

$$\begin{aligned} \rho_{11} &= \mathcal{E}_4 \cos^2 \theta + \mathcal{E}_3 \sin^2 \theta, \quad \rho_{22} = \mathcal{E}_0 \cos^2 \theta + \mathcal{E}_5 \sin^2 \theta, \\ \rho_{33} &= \mathcal{E}_6 \cos^2 \theta + \mathcal{E}_0 \sin^2 \theta, \quad \rho_{44} = \mathcal{E}_1 \cos^2 \theta + \mathcal{E}_2 \sin^2 \theta \\ \rho_{23} &= \rho_{32} = \mathcal{E}_0 \sin \theta \cos \theta, \end{aligned} \tag{14}$$

where

$$\mathcal{E}_0 = \Theta \sum_{a,b} \frac{\varkappa_A^a \varkappa_B^b}{\Upsilon_{ab}}, \tag{15}$$

$$\mathcal{E}_1 = \Theta |\mu_A|^2 \sum_{a,b} \frac{a \varkappa_A^a \varkappa_B^b}{\Upsilon_{ab}}, \tag{16}$$

$$\mathcal{E}_2 = \Theta |\mu_B|^2 \sum_{a,b} \frac{b \varkappa_A^a \varkappa_B^b}{\Upsilon_{ab}}, \tag{17}$$

$$\mathcal{E}_3 = \Theta |\mu_A|^2 \sum_{a,b} \frac{(a+1) \aleph_A^a \aleph_B^b}{\Upsilon_{ab}}, \tag{18}$$

$$\mathcal{E}_4 = \Theta |\mu_B|^2 \sum_{a,b} \frac{(b+1) \aleph_A^a \aleph_B^b}{\Upsilon_{ab}}, \tag{19}$$

$$\mathcal{E}_5 = \Theta |\mu_A|^2 |\mu_B|^2 \sum_{a,b} \frac{b(a+1) \aleph_A^a \aleph_B^b}{\Upsilon_{ab}}, \tag{20}$$

$$\mathcal{E}_6 = \Theta |\mu_A|^2 |\mu_B|^2 \sum_{a,b} \frac{a(b+1) \aleph_A^a \aleph_B^b}{\Upsilon_{ab}}, \tag{21}$$

$$\Theta = (1 - \aleph_A)(1 - \aleph_B), \tag{22}$$

$$\begin{aligned} \Upsilon_{ab} = & \cos^2\theta [1 + a|\mu_A|^2 + (b+1)|\mu_B|^2 \\ & + a(b+1)|\mu_A|^2|\mu_B|^2] + \sin^2\theta [1 + b|\mu_B|^2 \\ & + (a+1)|\mu_A|^2 + b(a+1)|\mu_A|^2|\mu_B|^2], \end{aligned} \tag{23}$$

$$\begin{aligned} & \mathcal{E}_0 + \cos^2\theta(\mathcal{E}_1 + \mathcal{E}_4 + \mathcal{E}_6) \\ & + \sin^2\theta(\mathcal{E}_2 + \mathcal{E}_3 + \mathcal{E}_5) = 1. \end{aligned} \tag{24}$$

Here,  $\aleph_A$  and  $\aleph_B$  are the mixed degree defined in Eq. (4) [55].  $\mu_A$  and  $\mu_B$  are the inner product of the mode functions defined by  $\mu = \langle \Gamma_q^*, \chi_{k0} \rangle$  [55,61]. Notably, the Eq. (13) and all results of our work are valid in the scenarios that one only considers the coupling between the detector qubit and the mode  $\mathbf{k}_0$ , and neglects the coupling between the detector qubit and other field modes.

### 3 The quantum resources of bipartite-qubit detectors subjected to scalar fields in an expanding spacetime

#### 3.1 The characterizations of QC, QD, BN, and NAQC

In this section, we first characterize QC in the expansion spacetime by using the relative entropy of coherence. QC is a fundamental quantum resource. QC of a quantum state is defined as the shortest distance from it to all incoherent states. Therefore, QC depends on the definition of incoherent state. However, the definition of incoherent state is dependent on the reference basis. One can use various avenues to measure QC of system based on the framework of Baumgratz et al. [2]. Thus, QC is a basis dependent quantity. The relative entropy of coherence is one of the important methods for quantifying QC [2]. The relative entropy of coherence of any two-qubit state  $\rho$  is defined as  $QC(\rho) = S(\rho_{diag}) - S(\rho)$  [2], where  $\rho_{diag}$  is the matrix containing only diagonal elements of  $\rho$  in the reference basis, and  $S(\rho) = -Tr(\rho \log_2 \rho)$  is the von Neumann entropy. Under the  $\sigma_z$ -representation, the incoherent state is the simple matrix that only contains the diagonal elements when choosing the eigenstates of  $\sigma_z$  as the reference bases. However, the incoherent state does not have this simple form when choosing the eigenstates of  $\sigma_x$  or  $\sigma_y$  as

the reference bases under the  $\sigma_z$ -representation. Therefore, researchers are accustomed to choosing the eigenstates of  $\sigma_z$  as the reference bases in experiment and theory [82–86]. For this reason, we choose the eigenstates of  $\sigma_z$  as the reference bases in this paper. Based on the Eq. (13), we can obtain QC of  $\rho_{AB}$ , namely

$$QC(\rho_{AB}) = \frac{1}{2\text{Ln}2} [A + B_- C_- + B_+ C_+] \tag{25}$$

with

$$\begin{aligned} A = & -2(\mathcal{E}_6 \cos^2\theta + \mathcal{E}_0 \sin^2\theta) \text{Ln}(\mathcal{E}_6 \cos^2\theta + \mathcal{E}_0 \sin^2\theta) \\ & -2(\mathcal{E}_0 \cos^2\theta + \mathcal{E}_5 \sin^2\theta) \text{Ln}(\mathcal{E}_0 \cos^2\theta + \mathcal{E}_5 \sin^2\theta), \end{aligned} \tag{26}$$

$$B_- = (\mathcal{E}_0 + \mathcal{E}_6) \cos^2\theta + (\mathcal{E}_0 + \mathcal{E}_5) \sin^2\theta - \sqrt{R}, \tag{27}$$

$$\begin{aligned} C_- = & -\text{Ln}2 + \text{Ln}\{(\mathcal{E}_0 + \mathcal{E}_6) \cos^2\theta \\ & + (\mathcal{E}_0 + \mathcal{E}_5) \sin^2\theta - \sqrt{R}\}, \end{aligned} \tag{28}$$

$$B_+ = (\mathcal{E}_0 + \mathcal{E}_6) \cos^2\theta + (\mathcal{E}_0 + \mathcal{E}_5) \sin^2\theta + \sqrt{R}, \tag{29}$$

$$\begin{aligned} C_+ = & -\text{Ln}2 \\ & + \text{Ln}\{(\mathcal{E}_0 + \mathcal{E}_6) \cos^2\theta + (\mathcal{E}_0 + \mathcal{E}_5) \sin^2\theta + \sqrt{R}\}, \end{aligned} \tag{30}$$

$$\begin{aligned} R = & (\mathcal{E}_0 - \mathcal{E}_6)^2 \cos^4\theta \\ & + 2[\mathcal{E}_0(\mathcal{E}_0 + \mathcal{E}_5) + \mathcal{E}_6(\mathcal{E}_0 - \mathcal{E}_5)] \cos^2\theta \sin^2\theta \\ & + (\mathcal{E}_0 - \mathcal{E}_5)^2 \sin^4\theta. \end{aligned} \tag{31}$$

Next let us investigate QD of system. The nonclassical correlations are nontrivial in the field of quantum information, and it can be conventionally represented by QD [16,17]. If a system possesses QD but does not possess quantum entanglement, the system can also be used to implement quantum information tasks. QD of system is  $QD(\rho) = I(A : B) - C(\rho)$  [16,17]. The total correlation  $I(A : B)$  is  $I(A : B) = S(\rho_A) + S(\rho_B) - S(\rho)$ , The classical correlation is given by  $C(\rho) = \max_{\Pi_i^B} [S(\rho_A) - S_{\Pi_i^B}(\rho_{A|B})]$ , where  $\Pi_i^B$  is a group of possible positive-operator-valued measurements on particle B,  $S_{\Pi_i^B}(\rho_{A|B}) = \sum_i q_i S(\rho_i^A)$  represents the conditional entropy of qubit A, and  $\rho_i^A = \text{Tr}_B(\Pi_i^B \rho_{AB} \Pi_i^B) / \text{Tr}_{AB}(\Pi_i^B \rho_{AB} \Pi_i^B)$ . Due to the fact that the Eq. (13) is the form of the bipartite-qubit X-state, and we can use QD of the bipartite-qubit X-state [87–89] to reveal QD of  $\rho_{AB}$ , viz.,

$$QD(\rho_{AB}) = \min\{Q_1, Q_2\}, \tag{32}$$

$$Q_1 = H(\rho_{11} + \rho_{33}) + \sum_{i=1}^4 \lambda_i \log_2 \lambda_i + q_1, \tag{33}$$

and

$$Q_2 = H(\rho_{11} + \rho_{33}) + \sum_{i=1}^4 \lambda_i \log_2 \lambda_i + q_2. \tag{34}$$

Here,

$$H(x) = -x \log_2 x - (1-x) \log_2 (1-x), \tag{35}$$

$$\kappa = \sqrt{[1 - 2(\rho_{33} + \rho_{44})]^2 + 4(|\rho_{14}| + |\rho_{23}|)^2}, \tag{36}$$

$$q_1 = H((1 + \kappa)/2), \tag{37}$$

$$q_2 = -\sum_i \rho_{ii} \log_2 \rho_{ii} - H(\rho_{11} + \rho_{33}), \tag{38}$$

$\lambda_i (i = 1, 2, 3, 4)$  are the eigenvalues of  $\rho_{AB}$ , namely,

$$\lambda_1 = \frac{1}{2} \{ \mathcal{E}_0 + \mathcal{E}_6 \cos^2 \theta + \mathcal{E}_5 \sin^2 \theta - \sqrt{\varpi} \}, \tag{39}$$

$$\lambda_2 = \frac{1}{2} \{ \mathcal{E}_0 + \mathcal{E}_6 \cos^2 \theta + \mathcal{E}_5 \sin^2 \theta + \sqrt{\varpi} \}, \tag{40}$$

$$\lambda_3 = \frac{1}{2} \{ (\mathcal{E}_1 + \mathcal{E}_4) \cos^2 \theta + (\mathcal{E}_2 + \mathcal{E}_3) \sin^2 \theta - |(\mathcal{E}_1 - \mathcal{E}_4) \cos^2 \theta + (\mathcal{E}_2 - \mathcal{E}_3) \sin^2 \theta| \}, \tag{41}$$

$$\lambda_4 = \frac{1}{2} \{ (\mathcal{E}_1 + \mathcal{E}_4) \cos^2 \theta + (\mathcal{E}_2 + \mathcal{E}_3) \sin^2 \theta + |(\mathcal{E}_1 - \mathcal{E}_4) \cos^2 \theta + (\mathcal{E}_2 - \mathcal{E}_3) \sin^2 \theta| \} \tag{42}$$

with

$$\varpi = 4\mathcal{E}_0^2 \cos^2 \theta \sin^2 \theta + [(\mathcal{E}_6 - \mathcal{E}_0) \cos^2 \theta + (\mathcal{E}_0 - \mathcal{E}_5) \sin^2 \theta]^2. \tag{43}$$

BN is stronger than QC (or QD). That is to say, if BN exists in a system, then QC (or QD) must also exist in the system, but not vice versa. BN of two-qubit states  $\rho$  can be characterized by the violation of CHSH inequality, i.e.,  $|\langle B_{CHSH} \rangle_\rho| = |\text{Tr}(\rho B_{CHSH})| \leq 2$  [26]. Here,  $B_{CHSH} = \mathbf{a} \cdot \boldsymbol{\sigma} \otimes (\mathbf{b} + \mathbf{b}') \cdot \boldsymbol{\sigma} + \mathbf{a}' \cdot \boldsymbol{\sigma} \otimes (\mathbf{b} - \mathbf{b}') \cdot \boldsymbol{\sigma}$  is the Bell operator.  $\mathbf{a}$ ,  $\mathbf{a}'$ ,  $\mathbf{b}$  and  $\mathbf{b}'$  represent different unit vectors,  $\boldsymbol{\sigma} = (\sigma_x, \sigma_y, \sigma_z)$ . For an arbitrary two-qubit state

$$\rho = \frac{1}{4} \left( I \otimes I + \mathbf{r} \cdot \boldsymbol{\sigma} \otimes I + I \otimes \mathbf{s} \cdot \boldsymbol{\sigma} + \sum_{m,n=1}^3 t_{nm} \sigma_n \otimes \sigma_m \right), \tag{44}$$

$I$  is identity operator,  $\mathbf{r} = \text{Tr}(\rho \boldsymbol{\sigma} \otimes I)$ , and  $\mathbf{s} = \text{Tr}(\rho I \otimes \boldsymbol{\sigma})$ .  $t_{nm} = \text{Tr}(\rho \sigma_n \otimes \sigma_m)$  is the matrix elements of spin correlation matrix  $T$ . The  $|\langle B_{CHSH} \rangle_\rho| = |\text{Tr}(\rho B_{CHSH})|$  has a maximum  $B_{CHSH}^{Max}(\rho)$  when  $\mathbf{a}$ ,  $\mathbf{a}'$ ,  $\mathbf{b}$  and  $\mathbf{b}'$  obey the following conditions [90],

$$\mathbf{b} + \mathbf{b}' = 2 \cos \theta \mathbf{c}, \mathbf{b} - \mathbf{b}' = 2 \sin \theta \mathbf{c}', \tag{45}$$

$$\theta = \theta_{opt} = \arctan \frac{|T\mathbf{c}'|}{|T\mathbf{c}|}, \tag{46}$$

$$\mathbf{a} = \frac{T\mathbf{c}}{|T\mathbf{c}|}, \mathbf{a}' = \frac{T\mathbf{c}'}{|T\mathbf{c}'|}. \tag{47}$$

Here,  $\mathbf{c}$  and  $\mathbf{c}'$  are two eigenvectors corresponding to two larger eigenvalues of  $T^T T$ , respectively. For a two-qubit X state  $\rho_X$  (spin correlation matrix is  $T = \text{diag}(t_{11}, t_{22}, t_{33})$ ),

using the conditions of Eqs. (45)–(47), the maximum expected value of the Bell operator can be simply represented by [90]

$$B_{CHSH}^{Max}(\rho_X) = 2 \sqrt{\sum_{i=1}^3 t_{ii}^2 - \lambda_{\min}} \tag{48}$$

with  $t_{ii} = \text{Tr}[\rho_X \sigma_i \otimes \sigma_i]$  and  $\lambda_{\min} = \min\{t_{11}^2, t_{22}^2, t_{33}^2\}$ . BN of  $\rho_X$  can be detected if and only if  $B_{CHSH}^{Max}(\rho_X) > 2$ , and one can use

$$BN(\rho_X) = \text{Max} \{ 0, B_{CHSH}^{Max}(\rho_X) - 2 \} \tag{49}$$

to characterize BN. Thereby, BN of  $\rho_{AB}$  is

$$BN(\rho_{AB}) = \text{Max} \{ 0, \text{Max} \{ B_1, B_2 \} - 2 \} \tag{50}$$

with

$$B_1 = 4\sqrt{2} |\mathcal{E}_0| \cos \theta \sin \theta, \tag{51}$$

$$B_2 = 2\sqrt{B'}, \tag{52}$$

$$B' = 4\mathcal{E}_0^2 \cos^2 \theta \sin^2 \theta + [(-\mathcal{E}_0 + \mathcal{E}_1 + \mathcal{E}_4 - \mathcal{E}_6) \cos^2 \theta + (-\mathcal{E}_0 + \mathcal{E}_2 + \mathcal{E}_3 - \mathcal{E}_5) \sin^2 \theta]^2. \tag{53}$$

Finally, we characterize NAQC of  $\rho_{AB}$ . NAQC is a new quantum resource, which is revealed by implementing a local measurement on subsystem of a bipartite system. If a bipartite system possesses NAQC, then the upper bound of QC (for a single-qubit state) measured under a set of mutually unbiased bases can be punctured [30]. Supposing Alice and Bob share a bipartite state  $\rho$ . Alice chooses the Pauli matrices  $\sigma_i (i = x, y, x)$  and performs the corresponding measurement on her particle. The measurement operator and outcome are  $\Pi_i^a = [I + (-1)^a \sigma_i]/2$  and  $a \in \{0, 1\}$ , respectively. Subsequently, Bob chooses the other Pauli operators  $\sigma_j (j \neq i)$  to measure QC of the conditional states  $\rho_{B|\sigma_i^a}$  (the ensemble of Bob's conditional states  $\{p(a|\sigma_i) = \text{Tr}(\Pi_i^a \rho), \rho_{B|\sigma_i^a}\}$ ). By using the relative entropy of coherence, the average coherence of  $\rho_{B|\sigma_i^a}$  can be given by

$$\bar{C}_{re}^{\sigma_j}(\{p(a|\sigma_i), \rho_{B|\sigma_i^a}\}) = \sum_a p(a|\sigma_i) C_{re}^{\sigma_j}(\rho_{B|\sigma_i^a}) \tag{54}$$

with  $\rho_{B|\sigma_i^a} = \text{Tr}_A(\Pi_i^a \rho)/p(a|\sigma_i)$ .  $C_{re}^{\sigma_j}$  is the relative entropy of coherence measured in the eigenbasis of  $\sigma_j$ . Considering all measurement choices of Alice, NAQC [30] can be achieved if

$$C_{re}^{na}(\rho) = \frac{1}{2} \sum_{i,j,a,i \neq j} p(a|\sigma_i) C_{re}^{\sigma_j}(\rho_{B|\sigma_i^a}) > C_{re}^m \tag{55}$$

can be violated.  $C_{re}^m \approx 2.2320$ . Based on the Eq. (13), NAQC of  $\rho_{AB}$  is

$$NAQC(\rho_{AB}) = \text{Max} \left\{ 0, \sum_{i=x,y,z} C_{re}^i - 2.232 \right\}, \quad (56)$$

where

$$C_{re}^x = C_{re}^y = \frac{1}{2\text{Ln}2} \left\{ 2\sqrt{D}\text{arccoth} \left[ \frac{1}{\sqrt{D}} \right] - [(\mathcal{E}_4 + \mathcal{E}_6)\cos^2\theta + (\mathcal{E}_0 + \mathcal{E}_3)\sin^2\theta] \times \text{Ln}[(\mathcal{E}_4 + \mathcal{E}_6)\cos^2\theta + (\mathcal{E}_0 + \mathcal{E}_3)\sin^2\theta] - [(\mathcal{E}_0 + \mathcal{E}_1)\cos^2\theta + (\mathcal{E}_2 + \mathcal{E}_5)\sin^2\theta] \times \text{Ln}[(\mathcal{E}_0 + \mathcal{E}_1)\cos^2\theta + (\mathcal{E}_2 + \mathcal{E}_5)\sin^2\theta] + \text{Ln} \left[ \frac{1 - \sqrt{D}}{2} \right] + \text{Ln} \left[ \frac{1 + \sqrt{D}}{2} \right] \right\} \quad (57)$$

$$C_{re}^z = \frac{1}{\text{Ln}2} \left\{ (\mathcal{E}_6\cos^2\theta + \mathcal{E}_0\sin^2\theta) \times \text{Ln} \left[ \frac{2(\mathcal{E}_6\cos^2\theta + \mathcal{E}_0\sin^2\theta)}{(\mathcal{E}_1 + \mathcal{E}_6)\cos^2\theta + (\mathcal{E}_0 + \mathcal{E}_2)\sin^2\theta} \right] + (\mathcal{E}_1\cos^2\theta + \mathcal{E}_2\sin^2\theta) \times \text{Ln} \left[ \frac{2(\mathcal{E}_1\cos^2\theta + \mathcal{E}_2\sin^2\theta)}{(\mathcal{E}_1 + \mathcal{E}_6)\cos^2\theta + (\mathcal{E}_0 + \mathcal{E}_2)\sin^2\theta} \right] + (\mathcal{E}_4\cos^2\theta + \mathcal{E}_3\sin^2\theta) \times \text{Ln} \left[ \frac{2(\mathcal{E}_4\cos^2\theta + \mathcal{E}_3\sin^2\theta)}{(\mathcal{E}_0 + \mathcal{E}_4)\cos^2\theta + (\mathcal{E}_3 + \mathcal{E}_5)\sin^2\theta} \right] + (\mathcal{E}_0\cos^2\theta + \mathcal{E}_5\sin^2\theta) \times \text{Ln} \left[ \frac{2(\mathcal{E}_0\cos^2\theta + \mathcal{E}_5\sin^2\theta)}{(\mathcal{E}_0 + \mathcal{E}_4)\cos^2\theta + (\mathcal{E}_3 + \mathcal{E}_5)\sin^2\theta} \right] \right\}, \quad (58)$$

$$D = \mathcal{E}_0^2 + 2\mathcal{E}_0 \cos 2\theta [(\mathcal{E}_1 - \mathcal{E}_4 - \mathcal{E}_6)\cos^2\theta + (\mathcal{E}_2 - \mathcal{E}_3 + \mathcal{E}_5)\sin^2\theta] + [(\mathcal{E}_1 - \mathcal{E}_4 - \mathcal{E}_6)\cos^2\theta + (\mathcal{E}_2 - \mathcal{E}_3 + \mathcal{E}_5)\sin^2\theta]^2. \quad (59)$$

### 3.2 The influences of various cosmic parameters on QC, QD, BN, and NAQC

In order to explore the influences of the expansion rapidity on QC, QD, BN, and NAQC, we plot QC, QD, BN, and NAQC of the system as a function of  $\sigma$  in Fig. 1. One can reveal in Fig. 1a that QC, QD, BN, and NAQC start at different values. An increase in the expansion rapidity induces smooth degenerations in QC and QD. Of particular note is that QC and QD are invariant with various values of  $\sigma$  when the expansion rapidity reaches a critical value, signifying that the influences of rapidity expansion on QC and QD are weaker than the effects of rapidity expansion on BN and NAQC. In contrast, an increase in the expansion rapidity is responsible for rapid dissipation of BN and NAQC. Finally, BN and NAQC disappear at the corresponding critical value of rapidity, and one can only detect BN and NAQC at lower expansion rapidity. As demonstrated in Fig. 1b, the characteristics of QC, QD,

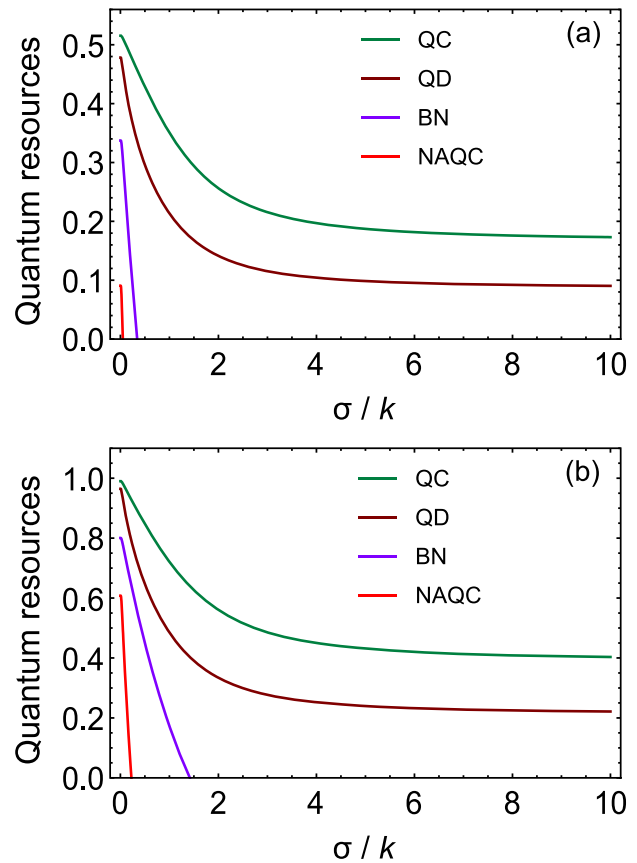


**Fig. 1** QC, QD, BN, and NAQC of the system with respect to the expansion rapidity  $\sigma$ . **a** is the results of  $\theta = 20^\circ$ , and **b** is the results of  $\theta = 45^\circ$ . For all graphs,  $\varepsilon = 19999.5$ ,  $\Omega = 2k$ ,  $\mu_A = \mu_B = 0.1$ ,  $m = 0.01k$ , and  $k = 1$

BN, and NAQC are similar to those in Fig. 1a when  $\theta = 45^\circ$  is considered as parameter of initial two-qubit state (namely maximally entangled state). Compared with the results in Fig. 1a, the change of the initial state weakens the effects of rapidity expansion on BN and NAQC, and BN and NAQC disappear at higher critical rapidity.

Now, we direct our attention to exploring the influences of  $\varepsilon$  on QC, QD, BN, and NAQC of bipartite-qubit detectors subjected to scalar fields in an expanding spacetime. Figure 2 displays the dependences of QC, QD, BN, and NAQC on the volume expansion, and these quantum resources start at different values. As found in Fig. 2a, the volume expansion does not influence QC, QD, BN, and NAQC. These quantum resources are invariant with different  $\varepsilon$ . Subsequently, QC, QD, BN, and NAQC decline with enhancing  $\varepsilon$ . NAQC is the most fragile, it vanishes before  $\varepsilon = \varepsilon_{\text{max}} = 19999.5$ , and BN disappears when  $\varepsilon = \varepsilon_{\text{max}} = 19999.5$ . Compared to the influences of volume expansion on BN and NAQC, the influences of volume expansion on QC and QD are weaker. Even if the volume increases to  $\varepsilon_{\text{max}} = 19999.5$ , the sudden deaths of QC and QD do not take place. If the state parameter

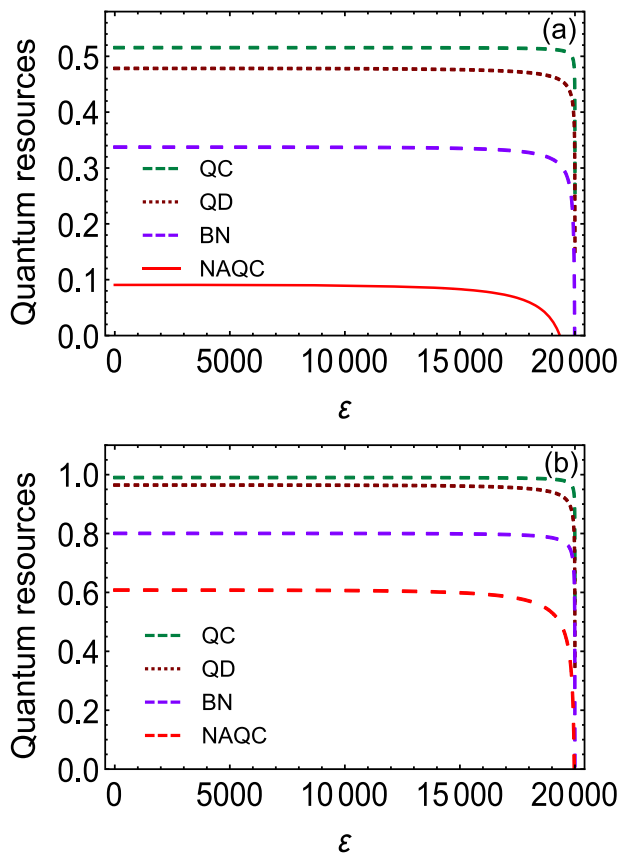


**Fig. 2** QC, QD, BN, and NAQC of the system with respect to the volume expansion  $\epsilon$ . **a** is the results of  $\theta = 20^\circ$ , and **b** is the results of  $\theta = 45^\circ$ . For all graphs,  $\sigma = 2k$ ,  $\Omega = 2k$ ,  $\mu_A = \mu_B = 0.1$ ,  $m = 0.01k$ , and  $k = 1$

$\theta = 45^\circ$  (as depicted in Fig. 2b), the influences of volume expansion on NAQC and BN are degenerative when  $0 < \epsilon < \epsilon_{\max}$ . The two quantum resources suddenly die only if the volume expansion of the cosmos reaches  $\epsilon_{\max}$ . In addition, QC and QD do not disappear when the volume expansion reaches the maximum. As a consequence, the increases of quantum resources in initial state can effectively attenuate the influences of volume expansion on QC, QD, BN, and NAQC.

Finally, we aim at examining the responsibilities of the particle mass of the scalar field for QC, QD, BN, and NAQC in Fig. 3. Here, we consider the strategy of  $\epsilon = \epsilon_{\max}$  due to the aforementioned results that the  $\epsilon_{\max}$  has remarkable influences on QC, QD, BN, and NAQC. It turns out that QC and QD start at different values. BN and NAQC start at zero for different critical values of  $m$ . QC, QD, BN, and NAQC increase with growing mass and eventually reach different fixed values as the mass continues to enhance. Of particular note is that BN and NAQC are very fragile under the effects of different particle masses of the scalar field. One can not witness BN and NAQC at smaller mass, even in the case of

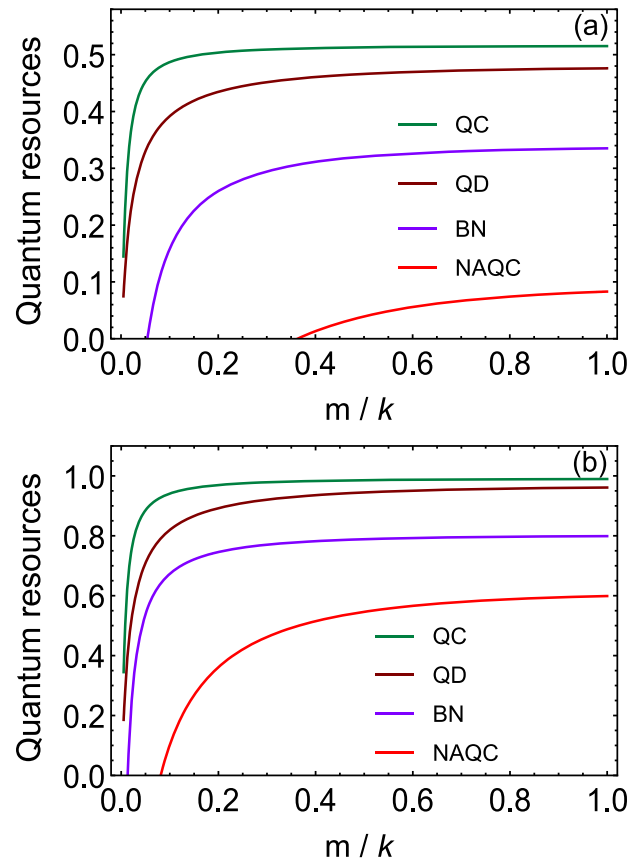


**Fig. 3** QC, QD, BN, and NAQC of the system with respect to the particle mass  $m$ . **a** is the results of  $\theta = 20^\circ$ , and **b** is the results of  $\theta = 45^\circ$ . For all graphs,  $\epsilon = \epsilon_{\max} = (\Omega^2/m^2 - 1)/2$ ,  $\sigma = 2k$ ,  $\Omega = 2k$ ,  $\mu_A = \mu_B = 0.1$ , and  $k = 1$

$\theta = 45^\circ$ . In contrast, QC and QD can be detected in case of different particle masses of the scalar field.

#### 4 Steering the quantum resources of bipartite-qubit detectors subjected to scalar fields in an expanding spacetime

From the results obtained in Sect. 3, one can reveal that the different cosmic parameters remarkably influence QC, QD, BN, and NAQC of bipartite-qubit detectors subjected to scalar fields in an expanding spacetime. Here, we come to increase QC, QD, BN, and NAQC of qubits detector subjected to scalar fields in an expanding spacetime through the local filtering operation. This operation is a non-trace-preserving map [91,92]

$$F = \begin{pmatrix} \sqrt{1-w} & 0 \\ 0 & \sqrt{w} \end{pmatrix} \tag{60}$$

with operator strength  $0 < w < 1$ . We implement the local filtering operation on qubit A of  $\rho_{AB}$ , and the output state is

$$\rho_{AB}^F = \begin{pmatrix} \rho_{11}^F & 0 & 0 & 0 \\ 0 & \rho_{22}^F & \rho_{23}^F & 0 \\ 0 & \rho_{32}^F & \rho_{33}^F & 0 \\ 0 & 0 & 0 & \rho_{44}^F \end{pmatrix} \tag{61}$$

with

$$\rho_{11}^F = \frac{(w - 1)(\mathcal{E}_4 \cos^2 \theta + \mathcal{E}_3 \sin^2 \theta)}{E}, \tag{62}$$

$$\rho_{22}^F = \frac{(w - 1)(\mathcal{E}_0 \cos^2 \theta + \mathcal{E}_5 \sin^2 \theta)}{E}, \tag{63}$$

$$\rho_{33}^F = \frac{-w(\mathcal{E}_6 \cos^2 \theta + \mathcal{E}_0 \sin^2 \theta)}{E}, \tag{64}$$

$$\rho_{44}^F = \frac{-w(\mathcal{E}_1 \cos^2 \theta + \mathcal{E}_2 \sin^2 \theta)}{E}, \tag{65}$$

$$\rho_{23}^F = \rho_{32}^F = -\frac{\mathcal{E}_0 \cos \theta \sin \theta \sqrt{(1 - w)w}}{E}, \tag{66}$$

$$E = \cos^2 \theta [(w - 1)\mathcal{E}_0 - \mathcal{E}_4 - w(\mathcal{E}_1 - \mathcal{E}_4 + \mathcal{E}_6)] - \sin^2 \theta [\mathcal{E}_3 + w(\mathcal{E}_0 + \mathcal{E}_2 - \mathcal{E}_3 - \mathcal{E}_5) + \mathcal{E}_5]. \tag{67}$$

QC of  $\rho_{AB}^F$  is

$$QC(\rho_{AB}^F) = \frac{1}{2\text{Ln}2} \left[ -\frac{F + G - J + K}{E} \right], \tag{68}$$

$$F = -2(w - 1)(\mathcal{E}_0 \cos^2 \theta + \mathcal{E}_5 \sin^2 \theta) \text{Ln} \left[ \frac{(w - 1)(\mathcal{E}_0 \cos^2 \theta + \mathcal{E}_5 \sin^2 \theta)}{E} \right], \tag{69}$$

$$G = 2w(\mathcal{E}_6 \cos^2 \theta + \mathcal{E}_0 \sin^2 \theta) \text{Ln} \left[ \frac{-w(\mathcal{E}_6 \cos^2 \theta + \mathcal{E}_0 \sin^2 \theta)}{E} \right], \tag{70}$$

$$J = \left[ (1 - w)\mathcal{E}_0 \cos^2 \theta + w\mathcal{E}_6 \cos^2 \theta + w\mathcal{E}_0 \sin^2 \theta + (1 - w)\mathcal{E}_5 \sin^2 \theta + \sqrt{J'} \right] \times \text{Ln} \left[ \frac{(-\mathcal{E}_0 + w\mathcal{E}_0 - w\mathcal{E}_6) \cos^2 \theta + (-w\mathcal{E}_0 - \mathcal{E}_5 + w\mathcal{E}_5) \sin^2 \theta - \sqrt{J'}}{2E} \right], \tag{71}$$

$$K = \left[ (w - 1)\mathcal{E}_0 \cos^2 \theta - w\mathcal{E}_6 \cos^2 \theta - w\mathcal{E}_0 \sin^2 \theta + (w - 1)\mathcal{E}_5 \sin^2 \theta + \sqrt{J'} \right] \times \text{Ln} \left[ \frac{(-\mathcal{E}_0 + w\mathcal{E}_0 - w\mathcal{E}_6) \cos^2 \theta + (-w\mathcal{E}_0 - \mathcal{E}_5 + w\mathcal{E}_5) \sin^2 \theta + \sqrt{J'}}{2E} \right], \tag{72}$$

$$J' = \left[ (\mathcal{E}_0 - w\mathcal{E}_0 + w\mathcal{E}_6) \cos^2 \theta + (\mathcal{E}_5 - w\mathcal{E}_5 + w\mathcal{E}_0) \sin^2 \theta \right]^2 + 4w(w - 1)(\mathcal{E}_0 \mathcal{E}_6 \cos^4 \theta + \mathcal{E}_5 \mathcal{E}_6 \cos^2 \theta \sin^2 \theta + \mathcal{E}_0 \mathcal{E}_5 \sin^4 \theta). \tag{73}$$

QD of  $\rho_{AB}^F$  is

$$QD(\rho_{AB}^F) = \min\{Q_1^F, Q_2^F\}, \tag{74}$$

$$Q_1^F = H(\rho_{11}^F + \rho_{33}^F) + \sum_{i=1}^4 \lambda_i^F \log_2 \lambda_i^F + q_1^F, \tag{75}$$

$$Q_2^F = H(\rho_{11}^F + \rho_{33}^F) + \sum_{i=1}^4 \lambda_i^F \log_2 \lambda_i^F + q_2^F, \tag{76}$$

$$q_1^F = H((1 + \kappa^F)/2), \tag{77}$$

$$\kappa^F = \sqrt{[1 - 2(\rho_{33}^F + \rho_{44}^F)]^2 + 4(|\rho_{14}^F| + |\rho_{23}^F|)^2}, \tag{78}$$

$$q_2^F = -\sum_i \rho_{ii}^F \log_2 \rho_{ii}^F - H(\rho_{11}^F + \rho_{33}^F), \tag{79}$$

$$\lambda_1^F = -\frac{w(\mathcal{E}_1 \cos^2 \theta + \mathcal{E}_2 \sin^2 \theta)}{E}, \tag{80}$$

$$\lambda_2^F = \frac{(w - 1)(\mathcal{E}_4 \cos^2 \theta + \mathcal{E}_3 \sin^2 \theta)}{E}, \tag{81}$$

$$\lambda_3^F = \frac{\varpi_-^F - \sqrt{J'}}{2E}, \tag{82}$$

$$\lambda_4^F = \frac{\varpi_+^F + \sqrt{J'}}{2E}, \tag{83}$$

$$\varpi_-^F = (-\mathcal{E}_0 + w\mathcal{E}_0 - w\mathcal{E}_6) \cos^2 \theta + (-w\mathcal{E}_0 - \mathcal{E}_5 - w\mathcal{E}_5) \sin^2 \theta, \tag{84}$$

$$\varpi_+^F = (-\mathcal{E}_0 + w\mathcal{E}_0 - w\mathcal{E}_6) \cos^2 \theta + (-w\mathcal{E}_0 - \mathcal{E}_5 + w\mathcal{E}_5) \sin^2 \theta. \tag{85}$$

BN of  $\rho_{AB}^F$  is

$$BN(\rho_{AB}^F) = \text{Max} \left\{ 0, \text{Max} \left\{ B_1^F, B_2^F \right\} - 2 \right\}, \tag{86}$$

$$B_1^F = 4\sqrt{\frac{2w(1 - w)\mathcal{E}_0^2 \cos^2 \theta \sin^2 \theta}{E^2}}, \tag{87}$$

$$B_2^F = 2\sqrt{\frac{4w(1 - w)\mathcal{E}_0^2 \cos^2 \theta \sin^2 \theta + E^2}{E^2}}. \tag{88}$$



NAQC of  $\rho_{AB}^F$  is

$$NAQC(\rho_{AB}^F) = \text{Max} \left\{ 0, \sum_{i=x,y,z} C_{re}^{i-F} - 2.232 \right\}, \quad (89)$$

where

$$\begin{aligned} C_{re}^{x-F} &= C_{re}^{y-F} \\ &= -\frac{1}{2E \text{Ln}2} \left\{ -2\sqrt{MN + N^2} \text{arccoth} \left[ \frac{E}{\sqrt{MN + N^2}} \right] \right. \\ &\quad + O \text{Ln} \left( \frac{O}{E} \right) + P \text{Ln} \left( \frac{P}{E} \right) - E \text{Ln} \left[ \frac{1}{2} - \frac{\sqrt{MN + N^2}}{2E} \right] \\ &\quad \left. - \text{Ln} \left[ 1 + \frac{\sqrt{MN + N^2}}{E} \right] \right\}, \quad (90) \end{aligned}$$

$$\begin{aligned} C_{re}^{z-F} &= \frac{1}{E \text{Ln}2} \left\{ -w(\mathcal{E}_6 \cos^2 \theta + \mathcal{E}_0 \sin^2 \theta) \right. \\ &\quad \times \text{Ln} \left[ \frac{2(\mathcal{E}_6 \cos^2 \theta + \mathcal{E}_0 \sin^2 \theta)}{(\mathcal{E}_1 + \mathcal{E}_6) \cos^2 \theta + (\mathcal{E}_0 + \mathcal{E}_2) \sin^2 \theta} \right] \\ &\quad - w(\mathcal{E}_1 \cos^2 \theta + \mathcal{E}_2 \sin^2 \theta) \\ &\quad \times \text{Ln} \left[ \frac{2(\mathcal{E}_1 \cos^2 \theta + \mathcal{E}_2 \sin^2 \theta)}{(\mathcal{E}_1 + \mathcal{E}_6) \cos^2 \theta + (\mathcal{E}_0 + \mathcal{E}_2) \sin^2 \theta} \right] \\ &\quad + (w - 1)(\mathcal{E}_4 \cos^2 \theta + \mathcal{E}_3 \sin^2 \theta) \\ &\quad \times \text{Ln} \left[ \frac{2(\mathcal{E}_4 \cos^2 \theta + \mathcal{E}_3 \sin^2 \theta)}{(\mathcal{E}_0 + \mathcal{E}_4) \cos^2 \theta + (\mathcal{E}_3 + \mathcal{E}_5) \sin^2 \theta} \right] \\ &\quad + (w - 1)(\mathcal{E}_0 \cos^2 \theta + \mathcal{E}_5 \sin^2 \theta) \\ &\quad \left. \times \text{Ln} \left[ \frac{2(\mathcal{E}_0 \cos^2 \theta + \mathcal{E}_5 \sin^2 \theta)}{(\mathcal{E}_0 + \mathcal{E}_4) \cos^2 \theta + (\mathcal{E}_3 + \mathcal{E}_5) \sin^2 \theta} \right] \right\}, \quad (91) \end{aligned}$$

$$M = \mathcal{E}_0^2 [(w - 1) \cos^2 \theta - w \sin^2 \theta]^2 - 2\mathcal{E}_0 [(w - 1) \cos^2 \theta + w \sin^2 \theta], \quad (92)$$

$$N = [-\mathcal{E}_4 + w(\mathcal{E}_1 + \mathcal{E}_4 - \mathcal{E}_6)] \cos^2 \theta + [-\mathcal{E}_3 + w(\mathcal{E}_2 + \mathcal{E}_3 - \mathcal{E}_5) + \mathcal{E}_5] \sin^2 \theta, \quad (93)$$

$$O = [(w - 1)\mathcal{E}_4 - w\mathcal{E}_6] \cos^2 \theta - [w(\mathcal{E}_0 - \mathcal{E}_3) + \mathcal{E}_3] \sin^2 \theta, \quad (94)$$

$$P = [(w - 1)\mathcal{E}_0 - w\mathcal{E}_1] \cos^2 \theta - [w(\mathcal{E}_2 - \mathcal{E}_5) + \mathcal{E}_5] \sin^2 \theta. \quad (95)$$

In order to reveal the influences of the filtering operation on various quantum resources of bipartite-qubit detectors subjected to scalar fields in an expanding spacetime, and realize the controls of these quantum resources, Fig. 4. characterizes the curves of QC, QD, BN, and NAQC with respect to the cosmic parameters ( $\sigma$ ,  $\varepsilon$ , and  $m$ ) under different operator strengths (no filtering operation,  $w = 0.6$ , and  $w = 0.9$ , respectively) of filtering operation. The solid curves are the results with no filtering operation. The dashed curves (dotted curves) are the results of  $w = 0.6$  ( $w = 0.9$ ). One can confirm in Fig. 4a that QC and QD are strengthened by implementing filtering operation. The higher operation strength ( $w = 0.9$ ) is responsible for more significant increases in QC and QD. It deserves to be emphasized that the effects of

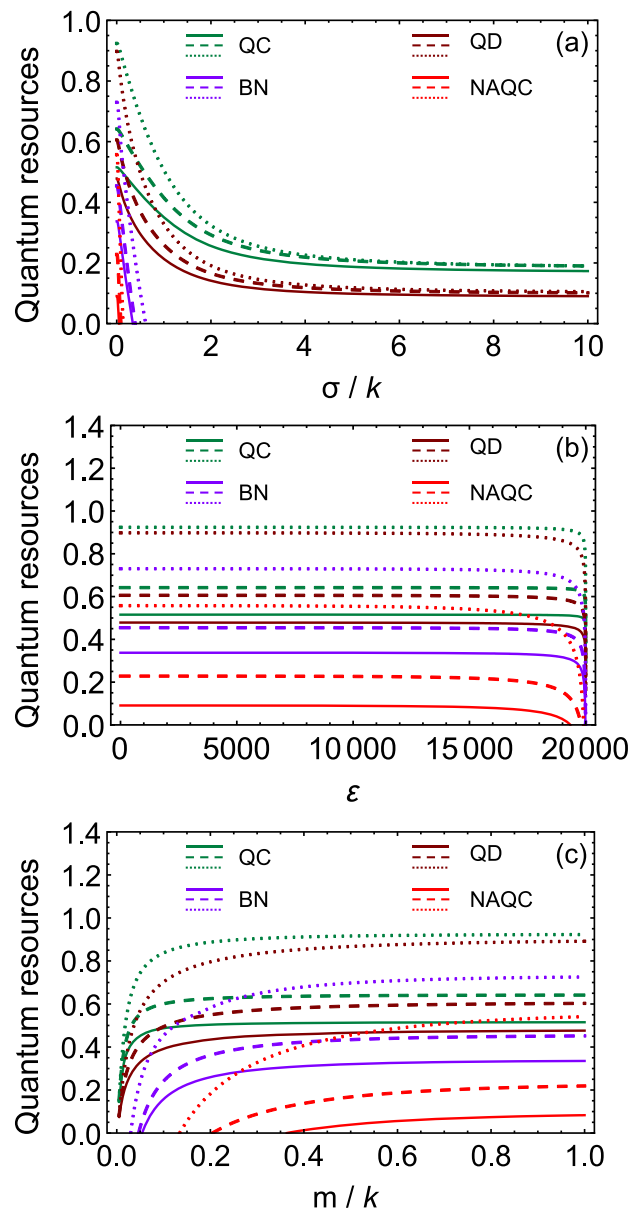


**Fig. 4** The results of QC, QD, BN, and NAQC under different operator strengths of the filtering operation. **a** is the results of  $\theta = 20^\circ$ ,  $\varepsilon = 19999.5$ ,  $\Omega = 2k$ ,  $\mu_A = \mu_B = 0.1$ , and  $m = 0.01k$ . **b** is the results of  $\theta = 20^\circ$ ,  $\sigma = 2k$ ,  $\Omega = 2k$ ,  $\mu_A = \mu_B = 0.1$ , and  $m = 0.01k$ . **c** is the results of  $\theta = 20^\circ$ ,  $\varepsilon = \varepsilon_{\text{max}} = (\Omega^2/m^2 - 1)/2$ ,  $\sigma = 2k$ ,  $\Omega = 2k$ , and  $\mu_A = \mu_B = 0.1$ . For all graphs,  $k = 1$ . The solid curves are the results with no filtering operation, the dashed curves are the results of  $w = 0.6$ , and the dotted curves are the results of  $w = 0.9$

the filtering operation on QC and QD degenerate as  $\sigma$  continues to grow. Even if  $w = 0.9$ , the influences of the filtering operation on QC and QD are not significant at higher rapidity, which are revealed by the green and brown dotted curves in Fig. 4a. As demonstrated by the purple (red) dashed curve and dotted curve in Fig. 4a, the filtering operation can effectively increase BN (NAQC) under different expansion rapidity, and thus can control the sudden death of BN (NAQC).

The stronger the  $w$ , the greater the critical rapidity of the sudden death is. It can be concluded in Fig. 4b that the filtering operation can also enhance QC, QD, BN, and NAQC in the process of volume expansion of the cosmos. Of particular note is that the operation can be used to avoid the disappearance of NAQC before the  $\varepsilon$  reaches the maximum, and the phenomena are uncovered by the red dashed curve and dotted curve in Fig. 4b. Besides, the filtering operation is ineffective in increasing QC, QD, BN, and NAQC if the volume reaches the maximum. By performing filtering operation with operation strength  $w = 0.6$  and  $w = 0.9$ , QC and QD enhance with different values of  $m$  in Fig. 4c. However, the smaller the mass, the less obvious the influence of filtration operation is. Fig. 4c also uncovers that the filtering operation can effectively steer and strengthen BN and NAQC. Significant for what follows, the filtration operation is responsible for the fact that BN and NAQC can be achieved at smaller particle mass, and the characteristics are illuminated by the purple and red dotted curve in Fig. 4c. That is to say, the decreases in quantum resources of bipartite-qubit detectors subjected to scalar fields in an expanding spacetime can be controlled and suppressed by implementing filtering operation on one of qubits.

## 5 Conclusions

To conclude, we have investigated the quantum resources of bipartite-qubit detectors subjected to scalar fields in an expanding spacetime. QC, QD, BN, and NAQC of the system are characterized, and the influences of different cosmic parameters on QC, QD, BN, and NAQC are explored. Moreover, we design the scenario that can be used to effectively increase the quantum resources of bipartite-qubit detectors subjected to scalar fields in an expanding spacetime. It can be concluded that an enlargement in expansion rapidity is responsible for reductions of QC, QD, BN, and NAQC. Among of them, the effects of the expansion rapidity on QC and QD are weaker, and they are invariant when the expansion rapidity reaches corresponding critical values. BN and NAQC sharply decline and then disappear at the corresponding critical rapidity. The invariant characteristics of QC, QD, BN, and NAQC appear in the process of volume expansion. After that, these quantum resources rapidly reduce as volume continues to expand. One can observe QC and QD in the interval of  $0 \leq \varepsilon \leq \varepsilon_{\max}$ . Nevertheless, NAQC and BN disappear when the volume expansion of cosmos approaches  $\varepsilon_{\max}$ . Considering  $\varepsilon = \varepsilon_{\max}$ , an increase in the particle mass of the scalar field results in enlargements of QC, QD, BN, and NAQC. Subsequently, these quantum resources are invariant with different values of mass. It is worth noting that BN and NAQC can not be captured when the particle mass of the scalar field is too small. With the help of the filtering opera-

tion, one can enhance the quantum resources of bipartite-qubit detector subjected to scalar fields in an expanding spacetime. Of particular note is that NAQC and BN can be detected at higher rapidity or smaller particle mass under the influence of the filtering operation, and these results can not be realized when we do not perform the filtering operation. The influences and controls of the filtering operation on QC, QD, BN, and NAQC are very significant at lower expansion rapidity, larger particle mass, and different volume expansions.

**Acknowledgements** This work was supported by the National Natural Science Foundation of China (Grant no. 12175001), a Natural Science Research Key Project of the Education Department of Anhui Province of China (Grant No. KJ2021A0943, 2022AH051681, and 2023AH052648), the Research Start-up Funding Project of High Level Talent of West Anhui University (Grant No. WGKQ2021048), an Open Project of the Key Laboratory of Functional Materials and Devices for Informatics of Anhui Higher Education Institutes (Grant No. FMDI202106), the University Synergy Innovation Program of Anhui Province (Project No. GXXT-2021-026), and the Anhui Provincial Natural Science Foundation (Grant Nos. 2108085MA18 and 2008085MA20).

**Data Availability Statement** This manuscript has no associated data or the data will not be deposited. [Authors' comment: There are no associated data available.]

**Open Access** This article is licensed under a Creative Commons Attribution 4.0 International License, which permits use, sharing, adaptation, distribution and reproduction in any medium or format, as long as you give appropriate credit to the original author(s) and the source, provide a link to the Creative Commons licence, and indicate if changes were made. The images or other third party material in this article are included in the article's Creative Commons licence, unless indicated otherwise in a credit line to the material. If material is not included in the article's Creative Commons licence and your intended use is not permitted by statutory regulation or exceeds the permitted use, you will need to obtain permission directly from the copyright holder. To view a copy of this licence, visit <http://creativecommons.org/licenses/by/4.0/>.

Funded by SCOAP<sup>3</sup>. SCOAP<sup>3</sup> supports the goals of the International Year of Basic Sciences for Sustainable Development.

## References

1. M.A. Nielsen, I.L. Chuang, *Quantum Computation and Quantum Information* (Cambridge University Press, Cambridge, 2000)
2. T. Baumgratz, M. Cramer, M.B. Plenio, *Phys. Rev. Lett.* **113**, 140401 (2014)
3. S. Luo, *Phys. Rev. Lett.* **91**, 180403 (2003)
4. D. Girolami, *Phys. Rev. Lett.* **113**, 170401 (2014)
5. C.S. Yu, *Phys. Rev. A* **95**, 042337 (2017)
6. C. Napoli, T.R. Bromley, M. Cianciaruso, M. Piani, N. Johnston, G. Adesso, *Phys. Rev. Lett.* **116**, 150502 (2016)
7. M. Piani, M. Cianciaruso, T.R. Bromley, C. Napoli, N. Johnston, G. Adesso, *Phys. Rev. A* **93**, 042107 (2016)
8. A. Streltsov, G. Adesso, M. Plenio, *Rev. Mod. Phys.* **89**, 041003 (2017)
9. M.L. Hu, X.Y. Hu, J.C. Wang, Y. Peng, Y.R. Zhang, H. Fan, *Phys. Rep.* **762–764**, 1 (2018)

10. T. Theurer, D. Egloff, L. Zhang, M.B. Plenio, Phys. Rev. Lett. **122**, 190405 (2019)
11. M.-L. Hu, Y.-Y. Gao, H. Fan, Phys. Rev. A **101**, 032305 (2020)
12. H. Yang, Z.-Y. Ding, X.-K. Song, H. Yuan, D. Wang, J. Yang, C.-J. Zhang, L. Ye, Phys. Rev. A **103**, 022207 (2021)
13. D. Patel, S. Patro, C. Vanarasa, I. Chakrabarty, A.K. Pati, Phys. Rev. A **103**, 022422 (2021)
14. Z. Ma, Z. Zhang, Y. Dai, Y. Dong, C. Zhang, Phys. Rev. A **103**, 012409 (2021)
15. D.Z. Rossatto, D.P. Pires, F.M. de Paula, O.P. de Sá Neto, Phys. Rev. A **102**, 053716 (2020)
16. H. Ollivier, W.H. Zurek, Phys. Rev. Lett. **88**, 017901 (2001)
17. L. Henderson, V. Vedral, J. Phys. A **34**, 6899 (2001)
18. L. Roa, J.C. Retamal, M. Alid-Vaccarezza, Phys. Rev. Lett. **107**, 080401 (2011)
19. B. Li, S.M. Fei, Z.X. Wang, H. Fan, Phys. Rev. A **85**, 022328 (2012)
20. B.P. Lanyon, M. Barbieri, M.P. Almeida, A.G. White, Phys. Rev. Lett. **101**, 200501 (2008)
21. J. Cui, H. Fan, J. Phys. A: Math. Theor. **43**, 045305 (2010)
22. T. Werlang, C. Trippe, G.A.P. Ribeiro, G. Rigolin, Phys. Rev. Lett. **105**, 095702 (2010)
23. R. Dillenschneider, Phys. Rev. B **78**, 224413 (2008)
24. J.S. Bell, Physics **1**, 195 (1965)
25. N. Brunner, D. Cavalcanti, S. Pironio, V. Scarani, S. Wehner, Rev. Mod. Phys. **86**, 419 (2014)
26. J.F. Clauser, M.A. Horne, A. Shimony, R.A. Holt, Phys. Rev. Lett. **23**, 880 (1969)
27. A.K. Ekert, Phys. Rev. Lett. **67**, 661 (1991)
28. Č. Brukner, M. Żukowski, J.W. Pan, A. Zeilinger, Phys. Rev. Lett. **92**, 127901 (2004)
29. S. Pironio, A. Acín, S. Massar, A.B. de la Giroday, D.N. Matsukevich, P. Maunz, S. Olmschenk, D. Hayes, L. Luo, T.A. Manning, C. Monroe, Nature **464**, 1021 (2010)
30. D. Mondal, T. Pramanik, A.K. Pati, Phys. Rev. A **95**, 010301(R) (2017)
31. D. Mondal, D. Kaszlikowski, Phys. Rev. A **98**, 052330 (2018)
32. M.L. Hu, X.M. Wang, H. Fan, Phys. Rev. A **98**, 032317 (2018)
33. M.L. Hu, H. Fan, Phys. Rev. A **98**, 022312 (2018)
34. S. Datta, A.S. Majumdar, Phys. Rev. A **98**, 042311 (2018)
35. Z.Y. Ding, H. Yang, H. Yuan, D. Wang, J. Yang, L. Ye, Phys. Rev. A **100**, 022308 (2019)
36. L. Wang, D. Bai, Y. Xia, W. Ho, Phys. Rev. Lett. **130**, 096201 (2023)
37. H.-L. Shi, S. Ding, Q.-K. Wan, X.-H. Wang, W.-L. Yang, Phys. Rev. Lett. **129**, 130602 (2023)
38. F. Mayo, A.J. Roncaglia, Phys. Rev. A **105**, 062203 (2022)
39. Q. Xiao, C. Wen, J. Jing, J. Wang, Eur. Phys. J. C **82**, 893 (2022)
40. X.K. Song, Y.Q. Huang, J.J. Ling, M.H. Yung, Phys. Rev. A **98**, 050302(R) (2018)
41. F. Ming, X.-K. Song, J. Ling, L. Ye, D. Wang, Eur. Phys. J. C **80**, 275 (2020)
42. Y.-W. Li, L.-J. Li, X.-K. Song, D. Wang, L. Ye, Eur. Phys. J. C **82**, 799 (2022)
43. D. Lacroix, A.B. Balantekin, M.J. Cervia, A.V. Patwardhan, P. Siwach, Phys. Rev. D **106**, 123006 (2022)
44. L.-J. Li, F. Ming, X.-K. Song, L. Ye, D. Wang, Eur. Phys. J. C **82**, 726 (2022)
45. J. Faba, V. Martín, L. Robledo, Phys. Rev. A **103**, 032426 (2021)
46. H. Wu, L. Chen, Phys. Rev. D **107**, 065006 (2023)
47. S.-M. Wu, Y.-T. Cai, W.-J. Peng, H.-S. Zeng, Eur. Phys. J. C **82**, 412 (2022)
48. J.L. Ball, I. Fuentes-Schuller, F.P. Schuller, Phys. Lett. A **359**, 550 (2006)
49. L. Parker, D. Toms, *Quantum Field Theory in Curved Spacetime* (Cambridge University Press, Cambridge, 2009)
50. I. Fuentes, R.B. Mann, E. Martín-Martínez, S. Moradi, Phys. Rev. D **82**, 045030 (2010)
51. S. Moradi, R. Pierini, S. Mancini, Phys. Rev. D **89**, 024022 (2014)
52. E. Martín-Martínez, N.C. Menicucci, Class. Quantum Gravity **31**, 214001 (2014)
53. H. Mohammadzadeh, Z. Ebadi, H. Mehri-Dehnavi, B. Mirza, R.R. Darabad, Quantum Inf. Process. **14**, 4787–4801 (2015)
54. X. Huang, J. Feng, Y.-Z. Zhang, H. Fan, Ann. Phys. N. Y. **397**, 336–350 (2018)
55. Y.J. Li, Y. Dai, Y. Shi, Eur. Phys. J. C **77**, 598 (2017)
56. X. Liu, J. Jing, J. Wang, Z. Tian, Quantum Inf. Process. **19**, 26 (2020)
57. H.A.S. Costa, P.R.S. Carvalho, Phys. Lett. A **126312**, 1047 (2020)
58. N.D. Birrell, P.C.W. Davies, *Quantum Fields in Curved Space* (Cambridge University Press, Cambridge, 1994)
59. C. Bernard, A. Duncan, Ann. Phys. (NY) **107**, 201 (1977)
60. H. Alexander, G. De Souza, P. Mansfield, I.G. Da Paz, M. Sampaio, EPL **115**, 10006 (2016)
61. W.G. Unruh, R.M. Wald, Phys. Rev. D **29**, 1047 (1984)
62. E. Adjei, K.J. Resch, A.M. Brańczyk, Phys. Rev. A **102**, 033506 (2020)
63. S. Onoe, T.L.M. Guedes, A.S. Moskalenko, A. Leitenstorfer, G. Burkard, T.C. Ralph, Phys. Rev. D **105**, 056023 (2022)
64. C. Gooding, S. Biermann, S. Erne, J. Louko, W.G. Unruh, J. Schmiedmayer, S. Weinfurter, Phys. Rev. Lett. **125**, 213603 (2020)
65. A. Svidzinsky, A. Azizi, J.S. Ben-Benjamin, M.O. Scully, W. Unruh, Phys. Rev. Lett. **126**, 063603 (2021)
66. W.B. Gao, P. Fallahi, E. Togan, J. Miguel-Sanchez, A. Imamoglu, Nature **491**, 426 (2012)
67. W.D. Oliver, F. Yamaguchi, Y. Yamamoto, Phys. Rev. Lett. **88**, 037901 (2002)
68. F.B. Basset, M. Valeri, E. Rocca, V. Muredda, D. Poderini, J. Neuwirth, N. Spagnolo, M.B. Rota, G. Carvacho, F. Sciarrino, R. Trotta, Sci. Adv. **7**, eabe6379 (2021)
69. M.C. Arnesen, S. Bose, V. Vedral, Phys. Rev. Lett. **87**, 017901 (2001)
70. G. Lagmago Kamta, Anthony F. Starace, Phys. Rev. Lett. **88**, 107901 (2002)
71. L. Campos Venuti, C. Degli Esposti Boschi, M. Roncaglia, Phys. Rev. Lett. **96**, 247206 (2006)
72. V. Menon, N.E. Sherman, M. Dupont, A.O. Scheie, D.A. Tennant, J.E. Moore, Phys. Rev. B **107**, 054422 (2023)
73. S. Shankar, M. Hatridge, Z. Leghtas, K.M. Sliwa, A. Narla, U. Vool, S.M. Girvin, L. Frunzio, M. Mirrahimi, M.H. Devoret, Nature **504**, 419 (2013)
74. D. Lachance-quirion, S.P. Wolski, Y. Tabuchi, S. Kono, K. usami, Y. Nakamura, Science **367**, 425 (2020)
75. S. Krastanov, H. Raniwala, J. Holzgrafe, K. Jacobs, M. Lončar, M.J. Reagor, D.R. Englund, Phys. Rev. Lett. **127**, 040503 (2021)
76. S.-B. Zheng, G.-C. Guo, Phys. Rev. Lett. **85**, 2392 (2000)
77. E. Solano, G.S. Agarwal, H. Walther, Phys. Rev. Lett. **90**, 027903 (2003)
78. Y. Zhou, S.Y. Xie, C.J. Zhu, Y.P. Yang, Phys. Rev. B **106**, 224404 (2022)
79. H. Jo, Y. Song, M. Kim, J. Ahn, Phys. Rev. Lett. **124**, 033603 (2020)
80. H. Levine, A. Keesling, A. Omran, H. Bernien, S. Schwartz, A.S. Zibrov, M. Endres, M. Greiner, V. Vuletić, M.D. Lukin, Phys. Rev. Lett. **121**, 123603 (2018)
81. C.-W. Yang, Y. Yu, J. Li, B. Jing, X.-H. Bao, J.-W. Pan, Nat. Photonics **16**, 658 (2022)
82. K.-D. Wu, Z. Hou, G.-Y. Xiang, C.-F. Li, G.-C. Guo, D. Dong, F. Nori, npj Quantum. Inf. **6**, 55 (2020)
83. Z.-Y. Ding, H. Yang, D. Wang, H. Yuan, J. Yang, L. Ye, Phys. Rev. A **101**, 032101 (2020)

84. L.-J. Li, F. Ming, X.-K. Song, L. Ye, D. Wang, *Eur. Phys. J. C* **82**, 726 (2022)
85. C. Radhakrishnan, Z. Lü, J. Jing, T. Byrnes, *Phys. Rev. A* **100**, 042333 (2019)
86. J. Wang, Z. Tian, J. Jing, H. Fan, *Phys. Rev. A* **93**, 062105 (2016)
87. Q. Chen, C. Zhang, S. Yu, X.X. Yi, C.H. Oh, *Phys. Rev. A* **84**, 042313 (2011)
88. C.Z. Wang, C.X. Li, L.Y. Nie, J.F. Li, *J. Phys. B: At. Mol. Opt. Phys.* **44**, 26 (015503)
89. S. Haddadi, M.R. Pourkarimi, A. Akhound, M. Ghominejad, *Mod. Phys. Lett. A* **34**, 1950175 (2019)
90. R. Horodecki, P. Horodecki, M. Horodecki, *Phys. Lett. A* **200**, 340 (1995)
91. M. Siomau, A.A. Kamli, *Phys. Rev. A* **86**, 032304 (2012)
92. T. Pramanik, Y.W. Cho, S.W. Han, S.Y. Lee, Y.S. Kim, S. Moon, *Phys. Rev. A* **99**, 030101(R) (2019)